

β -SiALON obtained from carbothermal reduction of kaolinite employing sample controlled reaction temperature (SCRT)

M. D. ALCALÁ, J. M. CRIADO, F. J. GOTOR, C. REAL*

Instituto de Ciencia de Materiales de Sevilla, c/Américo Vespucio s/n, Isla de La Cartuja, 41092 Sevilla, Spain

E-mail: creal@icmse.csic.es

Published online: 17 February 2006

β -SiALON has been obtained from carbothermal reduction of kaolinite by applying the sample controlled reaction temperature (SCRT) method. By using this technique for the synthesis it has been possible to obtain composites with different percentages of SiALON and with different microstructures. © 2006 Springer Science + Business Media, Inc.

1. Introduction

Many nonoxide ceramic materials have been studied because of they are potential candidates for special engineering applications due to their excellent mechanical properties, such as high strength, resistance to both thermal shock and wear, and chemical inertness at high temperature. The silicon nitride was the prime candidate, β -Si₃N₄ shows an excellent behavior at high temperature though it is rather difficult to sinter in order to get the theoretical density; additives such as MgO, CaO, Y₂O₃ or Al₂O₃ improve the sinterability and, in particular, alumina allows a solid solution to form through Si/Al and O/N substitutions. These substitutions in β -Si₃N₄ lead to a family of materials called β -SiALONs with a general formula Si_{6-z}Al_zO_zN_{8-z}. β -SiALONs show mechanical and thermal properties similar to those of β -Si₃N₄, but can be densified up to the theoretical density by heating at 1650°C in inert atmosphere. Sialon-based materials attracted great interest in the scientific community and in industry. Numerous applications using the combination of excellent properties have been published, such as metal-cutting and metal-forming tools, as inserts in gas-turbine engines, as porous ceramics in gas filter under high temperatures and corrosive environments, etc. [1–4]. Typically, SiALONs are prepared by firing powder compacts of Si₃N₄, AlN, and Al₂O₃ with some oxide sintering additives at high temperatures via a liquid phase sintering mechanism. Both the expensive starting powders and the complex manufacturing process have limited the practical application of SiALON ceramics. In order to reduce the manufacturing cost of SiALON products, investigations

have been performed to synthesize these materials on the basis of carbothermal reduction from clay, fly ash, which is a waste product from power plants, and coals, instead of relatively expensive synthetic powders [5–11]. The production of SiALON from aluminosilicates is analogous to the production of silicon nitride from silica. However, the reaction mechanism for the production of SiALON is more complex than that for silicon nitride and it has been shown that mechanical properties of SiALONs are governed by the combined effect of microstructure assemblage and secondary phase chemistry, each having a distinct contribution. In general it is accepted that the process takes place in three basic stages: thermal decomposition of kaolinite into mullite and vitreous silica, reduction of silica and formation of silicon carbide and reaction of carbon with silicon carbide and mullite to give β -SiALON. The first two stages are independent of the atmosphere, but the reaction rate of the second stage is a function of the carbon used, also the temperature, time reaction and impurities of the starting materials affect the intermediate and final product. The morphology seems to be influenced by many factors, starting powders, doping ions, compositions and probably synthesis conditions (the rate and composition of the gas flow, the kind of furnace employed, vertical or horizontal, the temperature and heating time, etc.) [12–16]. All these variables made difficult the interpretation and reproducibility of the results obtained from different authors. On the other hand, we have shown in previous papers [17–21] that the use of new method (SCRT), that permits a precise control of both the reaction rate and the concentration of the gas generated in the

*Author to whom all correspondence should be addressed.

reaction independently, allows us to tailor the microstructure of the obtained product. In this way, we have also prepared silicon nitride with controlled composition and morphology [20, 21]. The scope of present work is to use the SCRT method for preparing SiALONs from kaolinite and to compare the composition and morphology of the final products with the data reported in the literature.

2. Experimental

Kaolinite from Burela (Spain) with a specific area of 24 m²/g and active coal from Aldrich with a specific area of 1500 m²/g were used. A C/kaolinite mixture with a molar ratio of 5.3/1 has been used as raw material for the carbothermal synthesis of SiALONs. The residual carbon was removed by heating the samples at 600°C in air for 2 h.

The equipment developed for performing the carbothermal synthesis of SiALONs is constituted by a high temperature tubular furnace and a CO infrared (IR) sensor interfaced to the furnace temperature controller. The flowing gas (a mixture of 95% nitrogen + 5% hydrogen) sweeps the CO generated in the reaction through the IR detector and the temperature of the sample is controlled in such a way that the CO concentration remains constant at the value previously selected by the user. Moreover, the user can choose the reaction rate at every particular concentration of CO by properly selecting the flow rate of the reactive gas and the weight of the sample. Table I includes the experimental conditions for the two sets of experiments performed on the carbothermal reduction of kaolinite by the SCRT method.

The characterization of final products was accomplished by XRD, MAS NMR, and SEM. The XRD diagrams of the final products were recorded with a Philips diffractometer, model 1060 with CuK_α radiation and graphite monochromator. The percentages of different phases were determined using the expression of Sugahara *et al.* [22], $(\%i) = I_i / \sum I_i$. The dimensions of the coherently diffracting domains (crystallite size) of the β-SiALON were determined from the full-width at

half-maximum of the (201) XRD peak, using the Scherrer equation. Single-pulse MAS NMR measurements at 9.39 T were recorded on a Bruker DRX400 spectrometer. Powder samples were packed in 4 mm zirconia rotors and spun at 12 KHz. ²⁷Al spectra were acquired at a frequency of 104.26 MHz, using a π/4 pulse width of 4.5 μs and a delay time of 50 s for all the samples. ²⁹Si spectrum was acquired at a frequency of 79.49 MHz, using a π/6 pulse width of 2.66 μs and a delay time of 3.3 s. The chemical shifts are reported in ppm from 0.1 M solution of AlCl₃ and from tetramethylsilane, respectively. The SEM pictures of the samples were recorded with a Philips XL30 microscope at 30 KV, from samples ultrasonically dispersed in ethanol, supported on a metallic grill and covered with a thin graphite film.

3. Results and discussion

Fig. 1 shows the SCRT diagram for the carbothermal reduction of kaolinite under a gas flow rate of 200 cm³/min at a total pressure of 1 atm, corresponding to sample 3. The concentration of reaction-generated CO was kept constant at 5 × 10⁻³ atm throughout the experiment. The constant reaction rate, C, represents the fraction of solid reacted per minute and therefore, C⁻¹ accounts for the time at which carbothermal reduction of kaolinite is completed. From the SCRT diagram the reacted fraction, α, at time t, α(t), could be calculated. The α(t) value is given by the ratio between the area enclosed by the CO trace at time t and the total area when the reaction is over. In a previous article [20] we reported that the reacted fraction α could be calculated from the SCRT curves and plotted as a function of the temperature. It is well known [27] that the reaction rate of any solid state reaction is given by the

TABLE I Samples studied and synthesis conditions

| Sample | P _{CO} (atm) | Sample weigh (g) | Rate flow (cm ³ /min) (5%H ₂ + 95%N ₂) | C (min ⁻¹) |
|--------|-----------------------|------------------|--|------------------------|
| 1 | 0.0053 | 0.48 | 200 | 0.0067 |
| 2 | 0.0053 | 0.97 | 200 | 0.0030 |
| 3 | 0.0053 | 1.8 | 200 | 0.0015 |
| 4 | 0.0053 | 1.8 | 100 | 0.0009 |
| 5 | 0.0160 | 2 | 75 | 0.0016 |
| 6 | 0.0100 | 1.8 | 100 | 0.0015 |
| 3 | 0.0053 | 1.8 | 200 | 0.0015 |
| 7 | 0.0010 | 0.36 | 200 | 0.0015 |
| 8 | 0.0004 | 0.26 | 300 | 0.0013 |
| 9 | 0.0002 | 0.26 | 300 | 0.0007 |

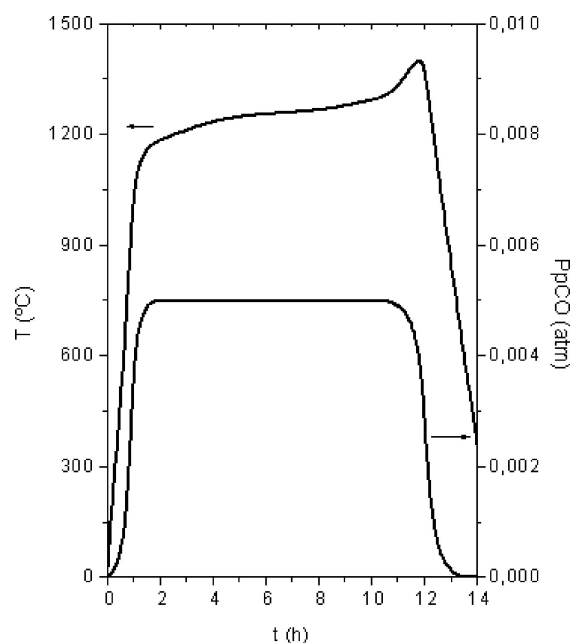


Figure 1 SCRT plot of the carbothermal reduction of kaolinite at 0.0053 atm of CO and a reaction rate of 0.0015 min⁻¹.

TABLE II Results of XRD studies: phase analysis of the crystalline phases present and the crystallite sizes for the SiALON phase

| Sample | D (nm) | Composition % | | | | |
|--------|----------|-----------------|---|--|-----|-----|
| | | β -SiALON | β -Si ₃ N ₄ | α -Si ₃ N ₄ | AlN | SiC |
| 1 | 25 | 50 | 9 | – | 6 | 35 |
| 2 | 24 | 67 | 12 | 13 | 9 | – |
| 3 | 25 | 78 | – | 10 | 12 | – |
| 4 | 20 | 75 | – | 13 | 12 | – |
| 5 | 24 | 65 | 16 | 10 | 8 | – |
| 6 | 25 | 65 | 15 | 10 | 10 | – |
| 7 | 21 | 74 | – | 16 | 10 | – |
| 8 | 25 | 64 | 12 | 17 | 7 | – |
| 9 | – | 44 | 31 | 14 | 11 | – |

following relationship: $d\alpha/dt = Ae^{-ER/T}f(\alpha)$, where A is the preexponential Arrhenius factor, E is the activation energy and $f(\alpha)$ is a function depending on the reaction mechanism. If the process is carried out at a constant reaction rate $C = d\alpha/dt$, the above equation can be rewritten in the form: $C = Ae^{-ER/T}f(\alpha)$. Thus, the higher the value of C , the higher could be the temperature at which a particular value of α is reached, provide that must be fulfilled. According to this statement, the α - T plot of reaction would move at higher temperatures by increasing the value of C , provided that the CO concentration surrounding the sample is maintained constant all over the experiment. In this way, the influence of the reaction temperature at any given CO concentration could be followed by recording a set of SCRT experimental data at different reaction rates, Table I. The first set (samples 1–4) corresponds to the experiments at constant pressure of CO and different reaction rate and the second one (samples 5–9) corresponds to the experiments carried out at constant reaction rate and different pressure of CO. The reproducibility of the α - T plots obtained at any given constant values of C and residual concentration of CO was very good and quite independent of starting sample weight and gas flow rate in the whole range investigated (0.3 to 6 g) and (70–300 cm³/min). Fig. 2a shows the $\alpha(t)$ - T plots under a CO residual concentration of 5×10^{-3} atm., and different reaction rates. It can be observed that the reaction occurred at higher temperatures when the value of the reaction rate was increased, provided that the CO concentration surrounding the sample was maintained constant throughout the experiment. Fig. 2b shows the influence of the CO concentration on the carbothermal reduction of kaolinite at a constant reaction rate, $C = 1.5 \times 10^{-3}$ min⁻¹. The α - T plot moved to higher temperature when the partial pressure of CO is increased.

All samples were characterized by XRD and their composition was calculated from the profiles: β -SiALON [(201), $d = 2.2169$ Å], β -Si₃N₄[(201), $d = 2.1799$ Å], α -Si₃N₄[(201), $d = 2.89$ Å], β -SiC[(220), $d = 1.54$ Å], and AlN [(101), $d = 2.37$ Å], using the expression of Sugahara *et al.* [22], (%) = $I_i / \sum I_i$. Table II includes the composition of the samples and the particle size of β -SiALON calculated by Shearrer

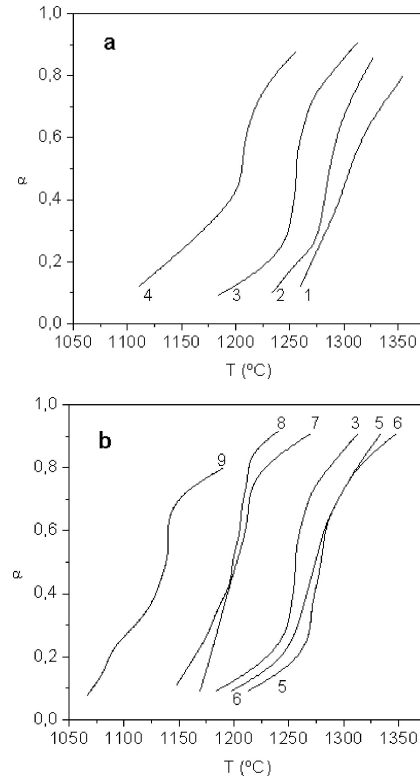


Figure 2 α - T plots calculated from the (SCRT) curves at (a) a pressure of 0.0053 atm of CO and different reactions rate. (b) a reaction rate of 0.0015 min⁻¹ and different pressures of CO.

equation. As can be observed, crystallite sizes are similar in all cases. For the first set of experiments (1–4), the composition of final products changes with the reaction rate used. These results together with Fig. 2a seem to demonstrate that the reaction temperature influences the composition of the final product. For the second set of experiments, (5–9), the composition of final products indicate that the percentage of β -SiALON increased from 66 to 78% when the CO concentration was decreased from 1.6×10^{-2} to 5.3×10^{-3} atm, and decreased from 78 to 44% when the CO concentration was decreased from 5.3×10^{-3} to 2×10^{-4} atm. From the above results we can conclude that the best conditions to obtain β -SiALON with the SCRT method are a partial pressure of CO = 0.005 atm and a reaction rate of 0.0015 min⁻¹, that correspond to sample 3, where the reaction occurs about 1250°C and is completed at about 1300°C. The data reported in the literature for the carbothermal synthesis of β -SiALONs do not show a complete agreement about the best conditions of temperature, heating time, gas flow, etc to achieve a high yield of this compound [6–7, 9–11, 15, 28–30]. Our preliminary studies with the same raw materials and equipment, using the isothermal method, see Table III, showed that the best conditions to obtain β -SiALON were $T = 1300^\circ\text{C}$, $t = 11$ h. The yielded was 54%. The samples were always composites of several phases including silicon nitride, aluminium nitride, silicon carbide and others sialons. These results are in good agreement with all

TABLE III Experimental conditions for the synthesis of SIALON by isothermal method and composition of final product

| T(°C) | th | Composition % | | | | | | |
|-------|----|-----------------|---|--|-----------|-----|-----|---------|
| | | β -SiALON | β -Si ₃ N ₄ | α -Si ₃ N ₄ | Others | AlN | SiC | Mullite |
| 1450 | 4 | — | 37 | — | 17, 16, 8 | 22 | ? | — |
| 1450 | 7 | — | 36 | — | 16, 13, 5 | 30 | ? | — |
| 1400 | 2 | 24 | 15 | — | ? | 13 | 48 | — |
| 1400 | 4 | 21 | 25 | — | ? | 16 | 37 | — |
| 1400 | 8 | 21 | 33 | — | ? | 22 | 24 | — |
| 1350 | 7 | 40 | 21 | — | — | 19 | 30 | — |
| 1350 | 4 | 41 | 29 | — | — | 13 | 18 | — |
| 1300 | 2 | 32 | 32 | — | — | — | 50 | 18 |
| 1300 | 6 | 42 | 28 | 6 | — | 8 | 16 | — |
| 1300 | 11 | 54 | 28 | 8 | — | 10 | — | — |
| 1200 | 6 | 31 | — | 14 | — | — | ? | 55 |
| 1200 | 11 | 37 | — | 23 | — | — | ? | 40 |

data previously reported in the literature. The high yield achieved in the present work, compared Tables II and III, shows the advantages of the SCRT method in front of isothermal method. This method allows to have a simultaneous control of the different experimental conditions that have any influence on the carbothermal reaction, like sample weight, gas flow rate, and temperature. This favors the production of α -SiALON, through the control of the reaction rate and partial pressure of CO, reducing the number of necessary experiments.

On the other hand, the composition of β -SiALON is represented by the formula $\text{Si}_{6-z}\text{Al}_z\text{O}_z\text{N}_{8-z}$, where z reaches a maximum of about 4.2. The values of z for the prepared samples were obtained from the X-ray diagrams by using the program L Sucreb for reticular lattice refinements, showing in all cases values of $z = 3$. Wild [31], in a study of production of β -SiALON from kaolin in ammonia-hydrogen atmosphere showed that the z value increases in the range of 1.07–1.83 when the temperature of reaction decreases. This behavior was not observed by us, but it is necessary to show that in Wild's study the reaction and the composition of the starting materials were different that those used in the present work and that the carbothermal reduction of kaolinite, as has been shown, is highly affected by the range of the temperature and the other experimental conditions employed.

Samples obtained from carbothermal reduction are composites of different phases as the X-ray data show. MAS NMR and XRD provide supplementary information about the composition of the samples. Solid-state ²⁷Al magic spinning (MAS) NMR spectroscopy offers a sensitive method of determining the coordination environments of aluminum in solid-state materials [23–26] which could complete the previous identification provided by X-ray analysis in our composite samples. On the other hand, ²⁹Si magic spinning (MAS) NMR spectroscopy does not evidence any difference between β -SiALON and β -Si₃N₄ but shows clearly the presence of SiC in the final stage of the reaction better than the X-ray diagram. In order to clarify the composition of selected samples ²⁷Al NMR (samples 1, 3 and 9) and ²⁹Si NMR (sample 1) spec-

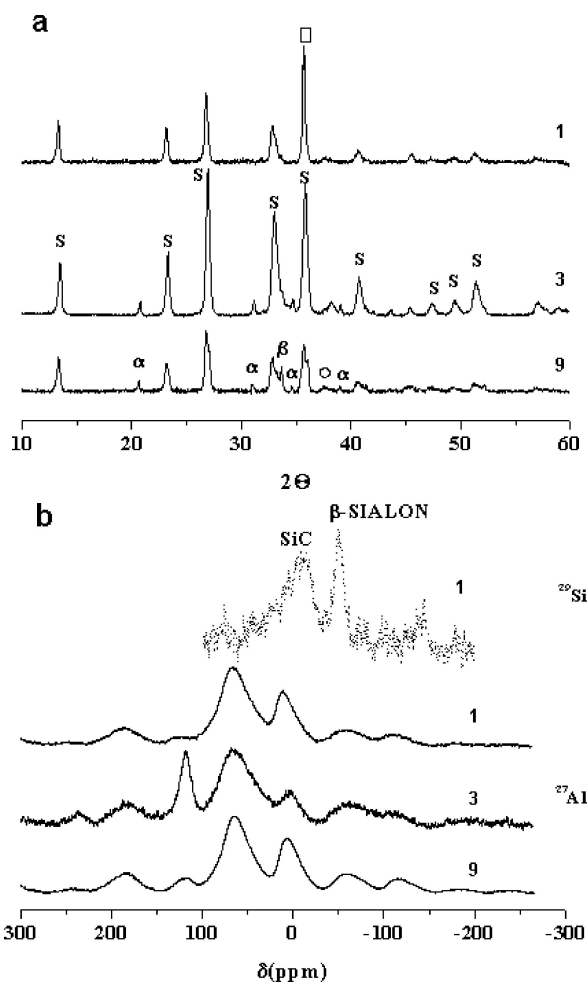


Figure 3 (a) XRD diffraction diagrams of the samples 1, 3 and 9. [β -SiALON), β (β -Si₃N₄), α (α -Si₃N₄), \square (SiC) and \circ (AlN)]. (b) ²⁷Al (SP) MAS NMR spectra of samples 1, 3 and 9; and ²⁹Si (SP) MAS NMR spectrum of sample 1.

troscopy was used. Fig 3a shows the X-ray patterns and Fig. 3b shows the NMR spectra for these samples. The ²⁷Al MASS-NMR spectra of samples 1, 3 and 9 show peaks in the position of about 66, 4 and 115 ppm. Peaks about 66 and 4 ppm are usually attributed to β -sialon,

and peak about 115 ppm to AlN. It has been reported in the literature that β -sialon shows three peaks at (4, 66 and 103–112 ppm). In our samples the last peak is not detected clearly, in agreement with Mackenzie *et al.* [32]. The resonance in β -SiALON could be broadened beyond detection due to distortion in the Al sites bonded to nitrogen. Sample 3, with the highest percentage of β -SiALON shows a large peak at 115 ppm that does not correspond with the AlN contents in the sample. In this case, it is possible that the peak corresponding to about 112 ppm of

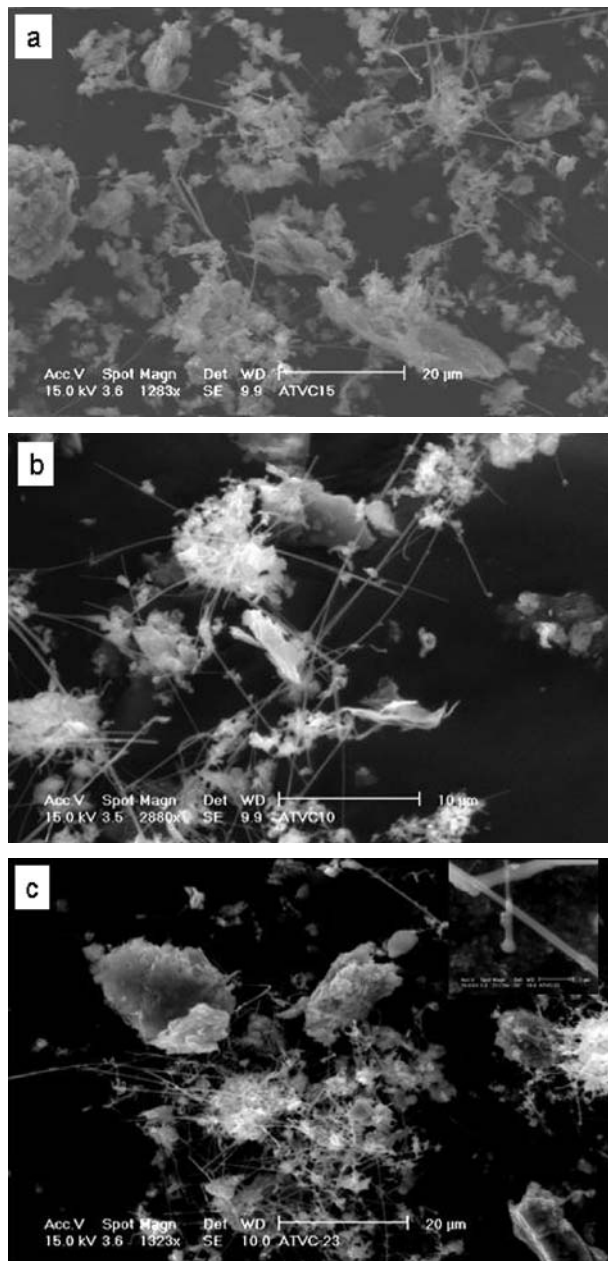


Figure 4 (a) SEM micrographs of sample 1, obtained by SCRT method at a pressure of CO = 0.0053 atm and a reaction rate of 0.0067 min^{-1} . (b) SEM micrographs of sample 3, obtained by SCRT method at a pressure of CO = 0.0053 atm and a reaction rate of 0.0015 min^{-1} . (c) SEM micrographs of sample 5, obtained by SCRT method at a pressure of CO = 0.0160 atm and a reaction rate of 0.0016 min^{-1} . Inset at droplet on the top of the whiskers high magnification.

sialon overlaps with the peak of about 115 ppm of AlN. In the ^{29}Si NMR spectrum of sample 1 we can clearly observe the peaks at -13 (SiC) and -49 (β -SiALON) ppm, respectively. This confirms the presence of SiC in this sample, not clear from the XRD data.

Fig. 4 shows the micrographs of samples 1, 3 and 5. All the samples exhibit non-uniform morphologies. Sample 1 (Fig. 4a), corresponding to the highest reaction rate is fundamentally constituted by particulates of different sizes and aspects. The EDAX analysis of this sample shows some particulates which only contain Si, and that could correspond to SiC. Sample 3 (Fig. 4b), with the highest yield of β -sialon, is more homogeneous than the others and is constituted by crystallites and whiskers, approximately, in the same proportion and with the smallest sizes. Micrograph of sample 5 (Fig. 4c), obtained at the highest CO pressure, shows higher proportion of whiskers, the crystallites have large sizes and the whiskers show droplets on the top (see the inset on the top of Fig. 4c); it is necessary to point out that the other samples show also droplets on the top of the whiskers but in a low percentage. These droplets are characteristic of the VLS mechanism but as has been shown by Wu *et al.* [33] in a study of the mechanism of formation of β -SiALON, the VS mechanism can not be excluded in the growth of the whiskers.

In summary, the use of the SCRT method allows obtaining composites with a higher yield of beta sialon than the isothermal method and reduces the number of necessary experiments to get it. The control of the reaction rate and the CO pressure could also allow obtaining samples with different morphology. The application of this method at the carbothermal reduction of other raw materials, halloysite, fly ash, coals etc, could enhance the SiALON contents in the obtained composites, in order to be applied industrially.

References

1. K. H. JACK, *J. Mater. Sci.* **11** (1976) 1135.
2. N. E. COTHER and P. HODGSON, *Trans. J. Br. Ceram. Soc.* **81** (1982) 141.
3. T. EKSTRÖM and M. NYGREN, *J. Am. Ceram. Soc.* **75**(2) (1992) 259.
4. J. F. YANG, Y. BEPPU, G. J. ZHANG, T. OHJI and S. KANZAKI, *ibid.* **85**(7) (2002) 1879.
5. F. K. VAN DIJEN and R. METSELAAR, *ibid.*, **68**(1) (1985) 16.
6. I. HIGGINS and A. HENDRY, *Br. Ceram. Trans. J.* **85** (1986) 161.
7. E. KOKMEIJE, C. SCHOLTE, F. BLÖMER and R. METSELAAR, *J. Mater. Sci.* **25** (1990) 1261.
8. C. ZHANG, K. KOMEYA, J. TATAMI, T. MEGURO and Y. B. CHENG, *J. Eur. Ceram. Soc.* **20** (2000) 1809.
9. J. E. GILBERT and A. MOSSET, *Mater. Res. Bull.* **32**(11) (1997) 1441.
10. F. J. NARCISO, A. LINARES-SOLANO and F. RODRIGUEZ-REINOSO, *J. Mater. Res.* **10**(3) (1995) 727.
11. A. A. KUDYBA-JANSEN, H. T. HINTZEN and R. METSELAAR, *Mater. Res. Bull.* **36** (2001) 1215.
12. F. YE, M. J. HOFFMAN, S. HOLZER, Y. ZHOU and M. IWASA, *J. Am. Cera. Soc.* **86**(12) (2003) 2136.
13. C. CHATFIELD, T. EKSTRÖM and M. MIKUS, *J. Mater. Sci.* **21** (1986) 2297.

14. L. BENCO, J. HAFNER, Z. LENCES and P. SAJGALIK, *J. Am. Ceram. Soc.* **86**(7) (2003) 1162.
15. F. J. NARCISO and F. RODRIGUEZ-REINOSO, *J. Mater. Chem.* **4**(7) (1994) 1137.
16. K. CHEN, M. E. F. L. COSTA, H. ZHOU and J. M. F. FERREIRA, *Mater. Chem. Phys.* **75** (2002) 252.
17. L. A. PÉREZ-MAQUEDA, J. M. CRIADO, J. SUBRT and C. REAL, *Catalysis Letters* **60** (1999) 151.
18. L. A. PÉREZ-MAQUEDA, J. M. CRIADO, C. REAL, J. SUBRT and J. BOHACEK, *J. Mater. Chem.* **9** (1999) 1839.
19. G. S. CHOPRA, C. REAL, M. D. ALCALÁ, L. A. PEREZ-MAQUEDA, J. SUBRT and J. M. CRIADO, *Chem. Mater.* **11** (1999) 1128.
20. M. D. ALCALÁ, J. M. CRIADO and C. REAL, *Adv. Eng. Mater.* **4**(7) (2002) 478.
21. C. REAL, M. D. ALCALÁ and J. M. CRIADO, *J. Am. Ceram. Soc.* **87**(1) (2004) 75.
22. Y. SUGAHARA, J. MIYAMOTO, K. KURODA and C. KATO, *App. Clay Sci.* **4** (1989) 11.
23. W. S. JUNG and S. K. AHN, *J. Mater. Sci. Letter* **16** (1997) 1573.
24. G. R. HATFIELD and K. R. CARDUNER, *J. Mater. Sci.* **24** (1989) 4209.
25. R. DUPREE, M. H. LEWIS and M. F. SMITH, *J. Appl. Cryst.* **21** (1988) 109.
26. J. SJÖRGGEG, R. K. HARRIS and D. C. APPERLEY, *J. Mater. Chem.* **2**(4) (1992) 433.
27. T. HATAKEYAMA and Z. LIU (eds). *Handbook of Thermal Analysis*, New York, J. Wiley & Sons, 1998, Chap. 3.
28. A. D. MAZZONI, E. E. AGLIETTI and E. PEREIRA, *J. Am. Ceram. Soc.* **76**(9) (1993) 2337.
29. S. A. SUVOROV, I. V. DOLGUSHEV and A. V. ZABOLOT-SKII, *Ref. Ind. Ceram.* **43**(3-4) (2002) 113.
30. J. YU, S. UENO, K. HIRAGUS, S. ZHANG and A. YAMAGUCHI, *J. Ceram. Soc. Japn.* **105** (1997) 880.
31. S. WILD, *J. Mater. Sci. Letter* **11**(10) (1976) 1972.
32. K. J. D. MACKENZIE, R. H. MEINHOLD, G. V. WHITE, C. M. SHEPPARD and B. L. SHERRIFF, *J. Mater. Sci.* **29** (1994) 2611.
33. Y. WU, H. ZHUANG, F. WU, D. DOLLIMORE, B. ZHANG, S. CHEN and W. LI, *J. Mater. Res.* **13**(1) (1998) 166.

*Received 15 February
and accepted 17 June 2005*